

# IR multiphoton depletion spectroscopy of metal cluster–ligand complexes

Benoit Simard<sup>a</sup>, Stéphane Dénoimée<sup>a</sup>, David M. Rayner<sup>a,\*</sup>,  
Deniz van Heijnsbergen<sup>b,c</sup>, Gerard Meijer<sup>b,c</sup>, Gert von Helden<sup>b</sup>

<sup>a</sup> *Steacie Institute for Molecular Sciences, National Research Council of Canada, 100 Sussex Drive, Ottawa, Ont., Canada K1A 0R6*

<sup>b</sup> *FOM-Institute for Plasma Physics Rijnhuizen, Edisonbaan 14, 3439 MN Nieuwegein, The Netherlands*

<sup>c</sup> *Department of Molecular and Laser Physics, University of Nijmegen, Toernooiveld, NL-6525 ED Nijmegen, The Netherlands*

Received 27 November 2001; in final form 1 March 2002

## Abstract

Free electron laser IR photodepletion spectroscopy of metal cluster–ligand complexes in a molecular beam is demonstrated on  $\text{Ag}_n(\text{NH}_3)_m$  complexes in the range 800–1150  $\text{cm}^{-1}$ . Where direct comparison can be made, our spectra agree with spectra measured by  $\text{CO}_2$  laser photodepletion spectroscopy. New vibrational spectroscopic data addressing previously unreachable spectral regions, including results for deuterated  $\text{ND}_3$  are reported for complexes of  $\text{Ag}_3$ ,  $\text{Ag}_4$  and  $\text{Ag}_5$ . © 2002 Published by Elsevier Science B.V.

## 1. Introduction

Infrared photodepletion experiments were first proposed as an approach to the infrared spectroscopy of metal cluster–ligand complexes by Cox and coworkers [1]. This early work, and later developments by Knickelbein and coworkers and by Rayner and Hackett and coworkers, has relied on using line tunable  $\text{CO}_2$  lasers to drive resonance enhanced multiphoton dissociation. With the very restricted wavelength coverage of the  $\text{CO}_2$  laser it has been possible to access only a few limited systems. These include the  $\delta_s$ -deformation mode of  $\text{NH}_3$  in  $\text{Ag}_n(\text{NH}_3)_m$  [2–4] and  $\text{Fe}_n(\text{NH}_3)_m$

[5], iron cluster hydride complexes [6], silver cluster–benzene complexes [7],  $\text{CH}_3\text{OH}$  on coinage metal clusters [8] and a comparative study of  $\text{Ag}_n(\text{C}_2\text{H}_4)_m$  and  $\text{Ag}_n(\text{C}_2\text{H}_4\text{O})_m$  [9]. For wide applicability and, especially, to access a range of model systems of significance to heterogeneous catalysis and other surface processes it is really necessary to have the ability to conduct such experiments throughout the chemical infrared.

An appropriately configured free electron laser (FEL) is clearly a candidate to provide such flexibility. High fluence and wide potential tunability are characteristics of FELs. FEL infrared spectroscopy has already had a remarkable success in cluster science through the measurement of the absorption spectrum of metal carbide clusters and their identification in circumstellar environments [10,11]. In this case absorption was detected

\* Corresponding author. Fax: +1-613-991-3437.

E-mail address: david.rayner@nrc.ca (D.M. Rayner).

through thermionic emission pumped by IR-REMPA in the metal carbide. Thermionic or delayed electron emission after UV excitation has been observed for a number of systems such as  $\text{Nb}_n$  [12], metallo-carbohedrenes [13], and  $\text{C}_{60}$  [14]. IR absorption measurements by exploiting thermionic emission is found to work for a surprisingly large amount of clusters including refractory metal carbide [10] and oxide clusters [15]. Nonetheless it is not a technique that can be applied generally as it requires high dissociation energies so that thermionic emission can compete with dissociation.

Depletion spectroscopy, on the other hand, is a general technique that has already been applied using a FEL to obtain infrared spectra of neutral and cationic aromatic hydrocarbons [16–19]. Note that, for cluster complexes, if the ligand itself is too strongly bound, it should generally be possible to co-attach a weakly bound marker molecule or rare gas atom, as done in these aromatic hydrocarbon studies and as demonstrated for  $\text{CO}_2$  laser PDS of iron hybrid clusters [6]. The FEL is untried in metal cluster–ligand complex depletion spectroscopy. Because its pulse characteristics (see Section 2) are very different from the  $\text{CO}_2$  lasers previously used for these studies it is not clear that sufficient depletion can be initiated by the FEL. Even on stable molecules there have only been a few studies on the mechanism of infrared multiphoton dissociation using FEL lasers [20,21].

This Letter reports on experiments carried out using the Free Electron Laser for Infrared experiments (FELIX) user facility at the FOM Institute for Plasma Physics ‘Rijnhuizen’ in the Netherlands to establish the feasibility of conducting IR photodepletion spectroscopy on metal cluster–ligand complexes. FELIX is uniquely configured for pulsed operation with wide tunability through the infrared. Using  $\text{Ag}_n(\text{NH}_3)_m$  complexes as a test bed we show that indeed the approach is feasible. Where direct comparison can be made, our spectra agree with spectra measured by  $\text{CO}_2$  laser PDS. We also report new spectroscopic data addressing previously unreachable spectral regions, including preliminary results on deuterated  $\text{ND}_3$  complexes.

## 2. Experimental

The molecular beam of  $\text{Ag}_n(\text{NH}_3)_m$  complexes is produced in a laser ablation cluster source by adding  $\text{NH}_3$  to the He carrier gas. As long as the ablation laser (frequency doubled Nd:YAG: Spectra-Physics GCR 150,  $\lambda = 532$  nm) is kept close to threshold for cluster production, this results in appreciable molecular complex formation as demonstrated below. The extent of  $\text{NH}_3$  complexation is controlled by adjusting the  $\text{NH}_3$  concentration in the He carrier gas.

FELIX delivers continuously tunable macropulses of infrared radiation of 20–80 mJ in energy and  $\sim 5$   $\mu\text{s}$  in duration at a repetition rate of 5 Hz. Each macropulse consists of a train of sub-nanosecond micropulses of  $\sim 10$   $\mu\text{J}$  in energy separated by 1 ns. In the cluster beam apparatus, which has been described previously [10,15], the beam is delivered in the optical arrangement shown in Fig. 1a. The FEL beam intersects the cluster beam at an angle of  $23^\circ$ . It is focused near the intersection with the cluster beam using a 75 mm focal length mirror and refocused back, but displaced to the side by 0.2 mm, by a second 37.5 mm focal length mirror. The IR beam diameter at the intersection is not known exactly due to the difficulty of placing

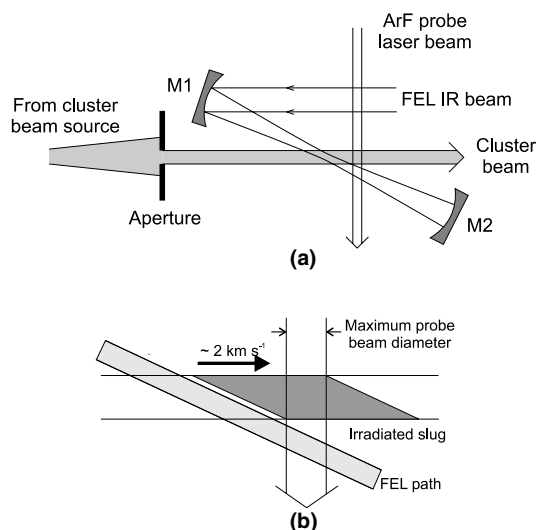


Fig. 1. Experimental arrangement and beam overlap details for FEL IR photodesorption.

the focus exactly in the molecular beam. It is in the range 60–200  $\mu\text{m}$ . Depletion experiments require the probe laser to interrogate as near as possible only clusters which have been fully exposed to the depletion laser. To fit the cluster beam to the FEL beamwaist, a 0.8 mm diameter aperture is placed 70 mm upstream of the interaction region where it provides a molecular beam diameter of 1 mm so that, with the side-by-side arrangement of the two foci, as much as possible of the entire cluster beam is exposed to FEL beam waist intensities. Because the cluster beam has a velocity of  $\sim 2 \text{ km s}^{-1}$  and the FEL macropulse is  $\sim 6 \mu\text{s}$  long the irradiated portion of the cluster beam is stretched over 12 mm. This reduces the maximum fluence which can be applied to the clusters proportionally. The ArF excimer probe laser (MPB Technologies,  $\lambda = 193 \text{ nm}$ ,  $\tau = 10 \text{ ns}$ ) is delayed until the depletion pulse is over to ensure full exposure. The probe laser intersects the cluster beam downstream from the FEL interaction region to allow for the movement of the irradiated portion of the beam during the FEL exposure. Its diameter is restricted so that, when timed correctly, it samples, as well as possible, only the portion of the cluster beam whose full width has been exposed to the FEL pulse, as shown in Fig. 1b. The intensity of the ArF probe is attenuated to the point that it does not, by itself, cause ion fragmentation through multiphoton processes.

Depletion spectra are measured by digitizing and automatically recording a series of TOF mass spectra at fixed wavelength intervals as the FEL is scanned incrementally under computer control. The spectra are constructed subsequently by integrating under the relevant mass gates. Apparent infrared photodepletion cross-sections are measured by recording mass spectra at a single FEL wavelength as a function of the FEL attenuation.

### 3. Results

We started the FEL photodepletion experiments by searching for depletion in the 1050–1100  $\text{cm}^{-1}$  region, where the earlier  $\text{CO}_2$  laser experiments located the  $\delta_s(\text{NH}_3)$  vibration of  $\text{Ag}_n(\text{NH}_3)_m$  complexes. The  $\delta_s(\text{NH}_3)$  deformation

of adsorbed  $\text{NH}_3$  correlates to the  $\nu_2$ -inversion, or ‘umbrella’ mode of free  $\text{NH}_3$  [22] and is expected to be the strongest IR transition in these complexes.

Fig. 2 compares mass spectra of silver cluster–ammonia complexes in the  $\text{Ag}_{4-5}$  cluster region taken with and without the FEL. The bottom trace, taken with ArF only shows collections of isotopomer peaks due to  $\text{Ag}_4\text{NH}_3$ ,  $\text{Ag}_4(\text{NH}_3)_2$ ,  $\text{Ag}_5$ ,  $\text{Ag}_5\text{NH}_3$  and  $\text{Ag}_5(\text{NH}_3)_2$ .  $\text{Ag}_4$  itself is not observed because its IP is higher than the 6.42 eV ArF photon energy [23]. Addition of a single  $\text{NH}_3$  molecule is sufficient to lower the IP so that its

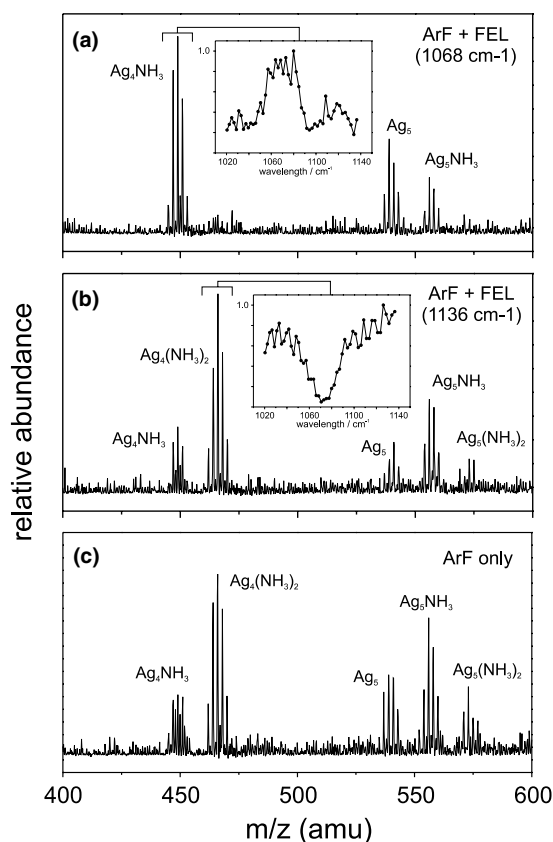


Fig. 2. Mass spectra of  $\text{Ag}_{4,5}(\text{NH}_3)_m$  clusters taken: (a) with the FEL tuned to  $1068 \text{ cm}^{-1}$  and (b)  $1136 \text{ cm}^{-1}$ , and (c) without the FEL. The isotopomer distributions associated with individual species reflect the natural abundance of the  $^{107}\text{Ag}$  and  $^{109}\text{Ag}$  isotopes. The inset in (a) shows the FEL wavelength dependence of the peaks due to  $\text{Ag}_4\text{NH}_3$  and in (b) that of the peaks due to  $\text{Ag}_4(\text{NH}_3)_2$ .

ammoniated complexes can be detected [4]. With the FEL tuned to  $1068\text{ cm}^{-1}$  and fired prior to the probe laser (top trace) the mass spectrum exhibits almost complete depletion of  $\text{Ag}_4(\text{NH}_3)_2$  and  $\text{Ag}_5(\text{NH}_3)_2$ . In addition,  $\text{Ag}_5\text{NH}_3$  is depleted by about half, while the  $\text{Ag}_4\text{NH}_3$  complex grows. It is clear that, at this wavelength,  $\text{Ag}_4(\text{NH}_3)_2$ ,  $\text{Ag}_5(\text{NH}_3)_2$  and  $\text{Ag}_5\text{NH}_3$  deplete significantly but that  $\text{Ag}_4\text{NH}_3$  does so little, if at all.

Comparison of the mass spectrum taken at  $1068\text{ cm}^{-1}$  (Fig. 2a) with that taken with the FEL tuned to  $1136\text{ cm}^{-1}$  (Fig. 2b), which shows no depletion, demonstrates a clear dependence on the FEL wavelength. Raw abundance spectra for  $\text{Ag}_4\text{NH}_3$  and  $\text{Ag}_4(\text{NH}_3)_2$  in the  $1020\text{--}1140\text{ cm}^{-1}$  region are shown in the insets of Fig. 2.  $\text{Ag}_4(\text{NH}_3)_2$  is depleted in the centre of this range with a correlated growth in  $\text{Ag}_4\text{NH}_3$ .

The infrared absorbance spectra of  $\text{Ag}_4\text{NH}_3$ ,  $\text{Ag}_5\text{NH}_3$ ,  $\text{Ag}_4(\text{NH}_3)_2$  and  $\text{Ag}_3(\text{NH}_3)_2$  obtained from such depletion spectra are shown in Fig. 3. The absorbance is calculated as  $-\ln(I/I_0)$ , where  $I$  is the abundance and  $I_0$  is the abundance at wavelengths where there is no depletion. To obtain the spectra of single  $\text{NH}_3$  complexes the ammonia

concentration was adjusted so that complexes with additional  $\text{NH}_3$  molecules adsorbed were not present.

In Fig. 3 we also compare the FEL absorbance spectrum of  $\text{Ag}_4(\text{NH}_3)_2$  with that obtained by  $\text{CO}_2$  laser depletion spectroscopy as depicted by the open circles. The  $\text{CO}_2$  laser experiments were carried out with a single transverse mode, single longitudinal mode pulse of  $\sim 100\text{ ns}$  duration main peak and a tail lasting  $1\text{ }\mu\text{s}$ . The FEL provides a train of sub-picosecond pulses of  $\sim 10\text{ }\mu\text{J}$  at  $1\text{ ns}$  separation, lasting  $\sim 5\text{ }\mu\text{s}$ . The bandwidths of the two sources are also very different. In medium sized molecules IR-REMPD absorptions are usually shifted to lower frequency compared to the corresponding low intensity absorptions [24]. This is because of the role anharmonicity plays in determining the efficiency of the adsorption of the additional few photons required to reach the quasi-continuum. The shift is also a function of the degree to which rotational relaxation and power broadening counter the rotational bottleneck. Because of the interplay of vibrational and rotational dynamics the position of IR-REMPD resonances in medium sized molecules can be sensitive to laser parameters such as intensity and pulse length [20,24]. In previous infrared photodepletion studies of metal cluster–ligand complexes it has been argued that the complexes are large enough, and the density of vibrational states is high enough, so that absorption of a single photon is sufficient to reach the quasi-continuum [25]. In this case, little difference is expected between the multiphoton and low intensity absorption spectrum.

The Ag–ammonia complexes studied here are not that large. However, our understanding of the IR-REMPD of Ag–ammonia complexes as produced in a molecular beam is that it is a low order process and probably involves single photon absorption for a significant proportion of the complexes in the beam [4]. This is because they are weakly bound species which are in equilibrium at room temperature before they are expanded. In this case we expect the IR-REMPD to be fluence driven and there to be no difference between the  $\text{CO}_2$  laser and FEL spectra. The relative agreement between the two spectra is consistent with this. In the  $\text{CO}_2$  laser case it was possible to ensure

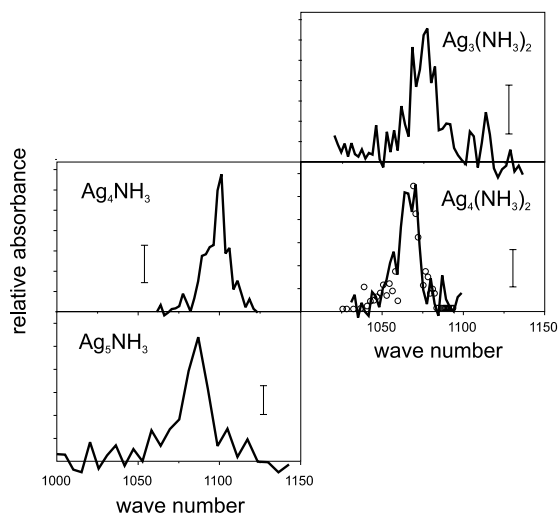


Fig. 3. Comparison of the infrared spectra of  $\text{Ag}_3(\text{NH}_3)_2$ ,  $\text{Ag}_4\text{NH}_3$ ,  $\text{Ag}_4(\text{NH}_3)_2$  and  $\text{Ag}_5\text{NH}_3$  in the  $\delta_s(\text{NH}_3)$  region as measured by FEL photodepletion. The scan interval was  $0.05\text{ }\mu\text{m}$ . The error bars indicate the magnitude of variations attributable to source fluctuations.

that the probe laser interrogated an ensemble of molecules which had experienced a well defined fluence. Absolute absorption cross-sections were obtained at individual laser lines from measurements of the intensity dependence of  $I/I_0$ . For the FELIX data, taken at a single intensity, we have scaled the absorbance to match the CO<sub>2</sub> laser data. With the proviso that the absorption process is fluence driven in both cases, the scaling factor we applied implies that overlap between the irradiated and probed volumes was not optimum in the present irradiation geometry, as discussed in Section 2. The indication is that sensitivity could be improved by an order of magnitude in future FEL desorption experiments by improving the overlap.

The infrared  $\delta_s(\text{NH}_3)$  peak frequencies, for the  $\text{Ag}_n(\text{NH}_3)_m$  complexes studied are given in Table 1. Also given in Table 1 are the frequencies assigned to  $\text{Ag}_n(\text{ND}_2\text{H})_m$  and  $\text{Ag}_n(\text{ND}_3)_m$ . We studied these species to demonstrate FEL photodepletion spectroscopy in a range inaccessible to the CO<sub>2</sub> laser and to determine the isotope shifts in the deformation mode. The complexes were generated by adding ND<sub>3</sub> to the He carrier gas in

place of NH<sub>3</sub>. Due to H/D exchange in the gas mixing system and source, this resulted in a mixture of deuterated and partly deuterated cluster complexes. In turn, this resulted in complex mass spectra from which we were only able to extract information on the clusters listed in the table.

In Fig. 4 we present infrared FEL photodepletion spectra attributable to the  $\delta_s(\text{ND}_3)$  mode of  $\text{Ag}_5\text{ND}_3$  (solid line) and the equivalent  $\delta(\text{ND}_2\text{H})$  mode of  $\text{Ag}_5\text{ND}_2\text{H}$ . In this case we were able to distinguish between mass spectral peaks due to the ND<sub>3</sub> and ND<sub>2</sub>H because the former show even displacement from the Ag<sub>5</sub> isotopomer peaks which are all spaced by 2 amu because the dominant Ag isotopes are <sup>107</sup>Ag and <sup>109</sup>Ag, present in almost equal abundance. For addition of a single ammonia molecule, only ND<sub>2</sub>H complexes can show odd displacement. There may be a contribution to the even displaced peaks from NDH<sub>2</sub> but we attribute the infrared band at 835 cm<sup>-1</sup> to the ND<sub>3</sub> complex because its position is close to that predicted by assuming the isotope shift is close to that found in gas phase ammonia [22] and to that reported for ND<sub>3</sub> adsorbed on an Ag(1 1 0)

Table 1  
 $\delta_s(\text{NH}_3)$ ,  $\delta(\text{ND}_2\text{H})$  and  $\delta_s(\text{ND}_3)$  deformation peak absorption frequencies (cm<sup>-1</sup>) of complexes of ammonia with small silver clusters

	NH <sub>3</sub>	ND <sub>2</sub> H	ND <sub>3</sub>	(NH <sub>3</sub> ) <sub>2</sub>	(ND <sub>2</sub> H) <sub>2</sub>	(ND <sub>3</sub> ) <sub>2</sub>
Ag <sub>2</sub>	1065 (115) <sup>a</sup> [1151 (119)]	–	–	–	–	–
Ag <sub>3</sub>	–	–	–	1075 (125) [1171 (139)]	–	–
Ag <sub>4</sub>	1100 (150) > 1090 <sup>b</sup> [S 1162 (130)] [L 1128 (96)]	–	–	1070 (120) 1065 <sup>b</sup> [SS 1141 (109)]	910 (97)	830 (84)
Ag <sub>5</sub>	1085 (135) 1082 <sup>b</sup>	920 (107)	835 (89)	–	–	–
Ag(1 1 0) <sup>c</sup>	1050		825			
Ag(3 1 0) <sup>d</sup>	1100					
Free ammonia <sup>e</sup>	950	813	746			

Experimental fundamental frequencies are from this work except where noted. The shifts compared to the mean of the inversion-split gas phase frequency of the free ligand are given in round brackets. The calculated values from DFT theory, [26], are shown in square brackets. S and L refer to two calculated isomers of Ag<sub>4</sub>NH<sub>3</sub> and SS refers to the stable isomer of Ag<sub>4</sub>(NH<sub>3</sub>)<sub>2</sub> see text and [26]. Also listed are  $\delta_s(\text{NH}_3)$  EELS frequencies for NH<sub>3</sub> adsorbed on Ag(1 1 0) and Ag(3 1 0) single crystal surfaces.

<sup>a</sup> Ref. [2].

<sup>b</sup> Ref. [4].

<sup>c</sup> Ref. [27].

<sup>d</sup> Ref. [28].

<sup>e</sup> Mean of the inversion doublet, Ref. [22].

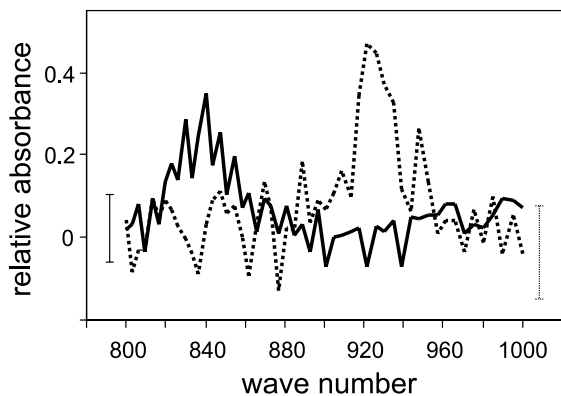


Fig. 4. Infrared FEL photodepletion spectra attributable to the  $\delta_s$ ND<sub>x</sub>H<sub>y</sub>-distortion mode of Ag<sub>5</sub>ND<sub>3</sub> (solid line) and Ag<sub>5</sub>ND<sub>2</sub>H. The scan interval was 0.05  $\mu$ m. The error bars indicate the magnitude of variations attributable to source fluctuations.

surface (825 cm<sup>-1</sup>) [27]. The band assigned to Ag<sub>5</sub>ND<sub>2</sub>H lies between the -ND<sub>3</sub> and -NH<sub>3</sub> positions, as expected.

In the case of Ag<sub>4</sub>(ND<sub>3</sub>)<sub>2</sub> and Ag<sub>4</sub>(ND<sub>2</sub>H)<sub>2</sub> it is impossible to assign the predominant isotopomer peaks to individual species because both complexes have even masses. Instead, in Fig. 5, we show the wavelength dependence of the sum of

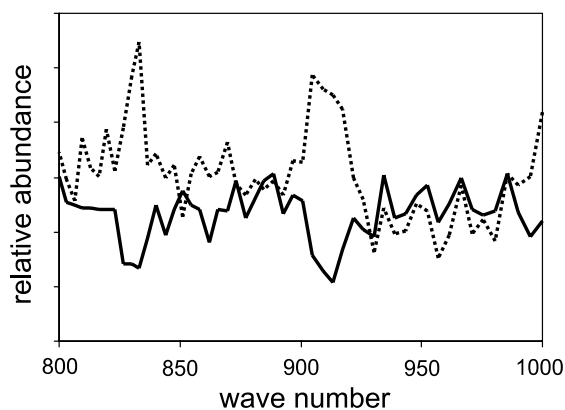


Fig. 5. Wavelength dependence of the infrared FEL photodepletion of mass spectral peaks which are indistinguishably due to a combination of Ag<sub>4</sub>(ND<sub>3</sub>)<sub>2</sub> and Ag<sub>4</sub>(ND<sub>2</sub>H)<sub>2</sub> (solid line) and the correlated growth of the sum of peaks due Ag<sub>4</sub>ND<sub>3</sub> and Ag<sub>4</sub>ND<sub>2</sub>H. The depletion at 830 cm<sup>-1</sup> is assigned to Ag<sub>4</sub>(ND<sub>3</sub>)<sub>2</sub> and that at 910 cm<sup>-1</sup> to Ag<sub>4</sub>(ND<sub>2</sub>H)<sub>2</sub>. The scan interval was 0.05  $\mu$ m.

isotopomer peaks which can only be assigned as mixtures of Ag<sub>4</sub>(ND<sub>3</sub>)<sub>2</sub> and Ag<sub>4</sub>(ND<sub>2</sub>H)<sub>2</sub> (with a possible contribution from Ag<sub>4</sub>(NDH<sub>2</sub>)<sub>2</sub>) and the sum of those which can be assigned to mixtures of Ag<sub>4</sub>ND<sub>3</sub> and Ag<sub>4</sub>ND<sub>2</sub>H. There is a correlation between depletion of the former and growth of the latter which shows the photodepletion is due either to loss of ND<sub>3</sub> from Ag<sub>4</sub>(ND<sub>3</sub>)<sub>2</sub> or ND<sub>2</sub>H from Ag<sub>4</sub>(ND<sub>2</sub>H)<sub>2</sub>. Because there are two clearly separated bands and because their positions are close to expected values it is reasonable to assign the lower energy one to Ag<sub>4</sub>(ND<sub>3</sub>)<sub>2</sub> and the higher one to Ag<sub>4</sub>(ND<sub>2</sub>H)<sub>2</sub>. The Ag<sub>4</sub>ND<sub>3</sub>/ND<sub>2</sub>H growth spectrum in Fig. 5 also has a contribution from depletion of the mixed complex Ag<sub>4</sub>ND<sub>3</sub>ND<sub>2</sub>H. Because the two salient features also correlate with the depletion spectrum of the odd mass peaks attributable to Ag<sub>4</sub>ND<sub>3</sub>ND<sub>2</sub>H we conclude that ND<sub>3</sub> and ND<sub>2</sub>H have the same deformation frequencies in this mixed cluster as they do in Ag<sub>4</sub>(ND<sub>3</sub>)<sub>2</sub> and Ag<sub>4</sub>(ND<sub>2</sub>H)<sub>2</sub>, respectively.

#### 4. Comparison with Ag<sub>n</sub>(NH<sub>3</sub>)<sub>m</sub> DFT predictions and surface studies

Table 1 summarises the  $\delta$ (NH<sub>3</sub>) frequencies for ammonia complexes of small silver clusters found by FEL photodepletion and compares them, where applicable, to our previous CO<sub>2</sub> laser measurements and to density functional theory (DFT) predictions. Apart from Ag<sub>2</sub>NH<sub>3</sub>, the frequencies reported in Table 1 are either previously unmeasured or improvements on the earlier measurements where the limited range of the CO<sub>2</sub> laser meant that peak positions had to be extrapolated. As a group they provide an almost complete set of data for comparison with the recent DFT calculations of Chan and Fournier [26] on Ag<sub>n</sub>NH<sub>3</sub> ( $n = 1-4$ ) and Ag<sub>4</sub>(NH<sub>3</sub>)<sub>2</sub>. Chan and Fournier report harmonic frequencies. Their comment that their harmonic frequencies are reasonably larger than the observed fundamentals by 5–10% still holds.

The DFT calculations predict two stable isomers of Ag<sub>4</sub>NH<sub>3</sub> differing by having the NH<sub>3</sub> ligand atop bound to an Ag atom situated on either the short (S) or long (L) diagonal of D<sub>2h</sub> Ag<sub>4</sub>. The S form is more stable but it is not immediately clear

that this isomer is the most abundant in our beam. It is not known if complex production in our source is under thermodynamic or kinetic control. From the difference between the calculated harmonic frequency and our measured fundamental frequency ( $62\text{ cm}^{-1}$  for the S form compared with  $28\text{ cm}^{-1}$  for the L form) it is reasonable to assign the observed absorption to  $\text{Ag}_4\text{NH}_3(\text{S})$  as the larger difference matches better that observed in the other complexes. Furthermore, under saturation conditions the depletion spectrum for  $\text{Ag}_4(\text{NH}_3)_2$  is sufficiently broadened to reach frequencies where we observe sequential depletion of photoproduct  $\text{Ag}_4\text{NH}_3$ . The action spectrum for the sequential depletion matches that found for  $\text{Ag}_4\text{NH}_3$  by direct depletion. The only stable calculated form of  $\text{Ag}_4(\text{NH}_3)_2$  has the SS structure, where the  $\text{NH}_3$  ligands are bound opposite each other across the short diagonal. Desorption of  $\text{NH}_3$  can be expected to lead to  $\text{Ag}_4\text{NH}_3(\text{S})$  as this process is the lowest energy channel.

It has been remarked that even the smallest silver ammonia complex,  $\text{Ag}_2\text{NH}_3$ , shares common features with  $\text{NH}_3$  adsorbed on Ag surfaces [2]. These features not only include its  $\delta_s(\text{ND}_3)$  frequency, which is within  $15\text{ cm}^{-1}$  of the EELS value for  $\text{NH}_3$  on  $\text{Ag}(1\ 1\ 0)$ , but also aspects of its ultraviolet and infrared laser dissociation dynamics, its atop binding geometry and its binding energy. The  $\delta_s(\text{ND}_3)$  frequencies of the larger cluster complexes reported in Table 1 continue this parallel. They all lie between the surface values for  $\text{Ag}(1\ 1\ 0)$ ,  $1050\text{ cm}^{-1}$  and  $\text{Ag}(3\ 1\ 0)$ ,  $1100\text{ cm}^{-1}$ . By comparison with both the surface experiments and with DFT calculations they are consistent with the binding being dominated by interaction with a single Ag atom. The differences between the clusters, which are relatively small compared to the overall shift from the umbrella mode of free  $\text{NH}_3$ , show that the  $\delta_s(\text{ND}_3)$  frequency is sensitive to subtleties of the local binding environment, just as on surfaces. DFT studies of  $\text{NH}_3$  binding at metal sites suggest a correlation between binding energy and the  $\delta_s(\text{ND}_3)$  frequency due to the contribution of the  $\text{NH}_3$  dipole to the bond. Because motion towards planar  $\text{NH}_3$  decreases the dipole moment, the umbrella deformation is restricted in the complex and the frequency rises. We do not ob-

serve such a correlation between the  $\delta_s(\text{ND}_3)$  frequencies given in Table 1 and the binding energies of  $\text{Ag}_2\text{NH}_3$ ,  $\text{Ag}_4\text{NH}_3$  and  $\text{Ag}_5\text{NH}_3$ , which are 16, 14 and  $8\text{ kcal mol}^{-1}$ , respectively [4]. This suggests the dipole interaction contributes to but does not dominate the binding, at least in the case of  $\text{Ag}_2\text{NH}_3$  and  $\text{Ag}_4\text{NH}_3$ . The binding in  $\text{Ag}_5\text{NH}_3$  is thought to be largely electrostatic [4], explaining the relatively high  $\delta_s(\text{ND}_3)$  frequency despite the low binding energy.

The deuterated complexes,  $\text{Ag}_5\text{ND}_2\text{H}$ ,  $\text{Ag}_5\text{ND}_3$ ,  $\text{Ag}_4(\text{ND}_2\text{H})_2$  and  $\text{Ag}_4(\text{ND}_3)_2$  are found to absorb close to where predicted from the associated isotope shifts in free ammonia and the measured frequencies. The blue shift of the deformation on binding  $\text{NH}_3$  to Ag clusters decreases roughly proportionally to the frequency of the vibration.

## 5. Dynamic range

The promise of FEL photodepletion spectroscopy is to access transitions throughout the infrared. We have demonstrated this with measurements of the previously inaccessible  $\delta_s(\text{NH}_3)$  transition in  $\text{Ag}_2\text{NH}_3$  and several  $\delta_s(\text{ND}_3)$  transitions of deuterated ammonia complexes. We would have liked to have identified other fundamental frequencies including, in an ideal experiment, the other ligand modes, the Ag–N stretch and rock modes and metal cluster skeleton modes. The DFT calculations predict the  $\text{NH}_3$  rocking mode with its harmonic frequency at  $\sim 520\text{ cm}^{-1}$  to be the next strongest after the  $\text{NH}_3$  deformation mode. A search for this absorption in  $\text{Ag}_4(\text{NH}_3)_2$  was unsuccessful. We attribute this to two factors: incomplete overlap of our probe and depletion beams and instability in the available cluster source.

As discussed above the present irradiation and probe geometries are a compromise. Individual clusters do not experience the full FEL fluence because the cluster beam velocity carries them through the FEL beam in less than 10% of the macropulse width. In addition the probe overlap may be open to improvement as indicated by comparison with  $\text{CO}_2$  laser results.

In the present experiments, however, the major factor limiting sensitivity is source stability. De-

pletion of > 30% is required for it to register under present source conditions. Adding the reagent gas with the He buffer gas requires the source to be operated close to threshold in order that the reagent survives the ablation plasma. Under these conditions the cluster source itself is relatively unstable. Forming the cluster complexes in a small flow reactor after the cluster source will allow the metal clusters to be produced under optimum conditions for stability. In addition, developments in the stability of the metal cluster source itself will also improve matters.

Dealing with both these factors, we anticipate that the next generation of these experiments will have the signal-to-noise enhanced so that the sensitivity will be increased by at least an order of magnitude and possibly two.

## 6. Conclusions

In these preliminary experiments we have demonstrated the use of the FEL for metal cluster photodepletion spectroscopy and have been able to provide new spectroscopic information on  $\text{Ag}_n(\text{NH}_3)_m$  complexes and their deuterated analogues. We have identified where improvements can be made to take advantage of the tunability of the FEL to access weaker transitions to provide more detailed structural information on metal cluster complexes and on any other species which can only be prepared as part of a distribution in a molecular beam. Better sensitivity is anticipated from ensuring complete overlap between the FEL and probe beam and in stabilising the cluster source. Source stability is often the limiting issue in photodepletion experiments. Finally the ultimate improvement would come from carrying out the depletion as an intracavity experiment in the FEL. Building an intracavity molecular beam facility is currently under consideration at the FOM-institute.

## Acknowledgements

We gratefully acknowledge the support by the Stichting voor Fundamenteel Onderzoek der Materie (FOM) in providing the required beam time

on FELIX and highly appreciate the skilful assistance by the FELIX staff, in particular Dr. A.F.G. van der Meer and Dr. W.C.M. Berden.

## References

- [1] M.R. Zakin, D.M. Brickman, D.M. Cox, K.C. Reichmann, D.J. Trevor, A. Kaldor, *J. Chem. Phys.* 85 (1986) 1198.
- [2] D.M. Rayner, L. Lian, R. Fournier, S.A. Mitchell, P.A. Hackett, *Phys. Rev. Lett.* 74 (1995) 2070.
- [3] D.M. Rayner, L. Lian, K. Athanassenas, B.A. Collings, R. Fournier, S.A. Mitchell, P.A. Hackett, *Surf. Rev. Lett.* 3 (1996) 649.
- [4] D.M. Rayner, K. Athanassenas, B.A. Collings, S.A. Mitchell, P.A. Hackett, in: J. Jelinek (Ed.), *Theory of Atomic and Molecular Clusters*, Springer Series in Cluster Physics, Springer, Berlin, 1999, p. 371.
- [5] K.A. Jackson, M.B. Knickelbein, G. Koretsky, S. Srinivas, *Chem. Phys.* 262 (2000) 41.
- [6] M.B. Knickelbein, G.M. Koretsky, K.A. Jackson, M.R. Pederson, Z. Hajnal, *J. Chem. Phys.* 109 (1998) 10692.
- [7] G.M. Koretsky, M.B. Knickelbein, *Chem. Phys. Lett.* 267 (1997) 485.
- [8] M.B. Knickelbein, G.M. Koretsky, *J. Phys. Chem. A* 102 (1998) 580.
- [9] G.M. Koretsky, M.B. Knickelbein, *J. Chem. Phys.* 107 (1997) 10555.
- [10] D. van Heijnsbergen, G. von Helden, M.A. Duncan, A.J.A. van Roij, G. Meijer, *Phys. Rev. Lett.* 83 (1999) 4983.
- [11] G. von Helden, A.G.G.M. Tielens, D. van Heijnsbergen, M.A. Duncan, S. Hony, L.B.F.M. Waters, G. Meijer, *Science* 288 (2000) 313.
- [12] B.A. Collings, A. Amrein, D.M. Rayner, P.A. Hackett, *J. Chem. Phys.* 99 (1993) 4174.
- [13] S.F. Cartier, B.D. May, A.W.J. Castleman, *J. Chem. Phys.* 104 (1996) 3423.
- [14] E.E.B. Campbell, G. Ulmer, I.V. Hertel, *Phys. Rev. Lett.* 67 (1991) 1986.
- [15] G. von Helden, A. Kirilyuk, D. van Heijnsbergen, B. Sartakov, M.A. Duncan, G. Meijer, *Chem. Phys.* 262 (2000) 31.
- [16] H. Piest, G. von Helden, G. Meijer, *J. Chem. Phys.* 110 (1999) 2010.
- [17] H. Piest, G. von Helden, G. Meijer, *Astrophys. J.* 520 (1999) L75.
- [18] H. Piest, J. Oomens, J. Bakker, G. von Helden, G. Meijer, *Spectrochim. Acta A* 57 (2001) 717.
- [19] R.G. Satink, H. Piest, G. von Helden, G. Meijer, *J. Chem. Phys.* 111 (1999) 10750.
- [20] J.L. Lyman, B.E. Newnam, J.W. Early, A.F.G. van der Meer, *J. Phys. Chem. A* 101 (1997) 49.
- [21] J. Oomens, A.J.A. van Roij, G. Meijer, G. von Helden, *Astrophys. J.* 542 (2000) 404.



- [22] G. Herzberg, *Molecular Spectra and Molecular Structure*, vol. 2, second edn., Van Nostrand, Princeton, 1945.
- [23] G. Alameddini, J. Hunter, D. Cameron, M.M. Kappes, *Chem. Phys. Lett.* 192 (1992) 122.
- [24] V.S. Letokhov, *Nonlinear Laser Chemistry*, Springer Series in Chemical Physics, Springer, Berlin, 1983.
- [25] M.B. Knickelbein, *J. Chem. Phys.* 104 (1996) 3517.
- [26] W.-T. Chan, R. Fournier, *Chem. Phys. Lett.* 315 (1999) 257.
- [27] J.L. Gland, B.A. Sexton, G.E. Mitchell, *Surf. Sci.* 115 (1982) 623.
- [28] S.T. Ceyer, J.T.J. Yates, *Surf. Sci.* 155 (1985) 584.